PREDICTING PROTECTIVE FILM BEHAVIOUR ON LOW CARBON STEEL

M.E. INMAN[1], R.M. SHARP[1], G.A. WRIGHT[2] AND P.T. WILSON[3]

[1]Department of Chemical and Materials Engineering, University of Auckland
[2]Department of Chemistry, University of Auckland
[3]New Zealand Institute for Industrial Research and Development, Wellington

SUMMARY - Magnetite and duplex iron sulphide-magnetite films have been grown in a autoclave at T = 160°C, and analysed using Electrochemical Impedance Spectroscopy and equivalent circuit theory. Corrosion rates obtained from the impedance data compared well with those derived from coupon weight losses. However, it was apparent that the mechanism of corrosion and passive film growth was different for each system. Therefore, the considerable body of knowledge on magnetite formation in high temperature aqueous environments, and the protection of carbon steel by that film, cannot be applied to the duplex iron sulphide-magnetite system.

1. INTRODUCTION

The corrosion performance of steam transmission lines fabricated of low carbon steel is largely dependent upon a film of corrosion product, which protects the surface from the corrosive geothermal condensate. In low H_2S gas environments, such as at the Wairakei geothermal field, the dominant corrosion product formed is magnetite (Braithwaite, 1979). However, in the high gas environment at the Ohaaki field, a duplex film of iron sulphide overlying a layer of magnetite develops (Borshevska et al, 1982). The influence of fluid composition on the degree of protection offered by magnetite is known from practical experience and from laboratory based research (Marshall and Hugill, 1957, Foster and Tombs, 1962). Mechanisms by which magnetite provides protection have been proposed (Potter and Mann, 1965, Robertson, 1989, MacDonald, 1992, Sato, 1989) and although universal agreement has not been reached, they do provide a rational basis for predicting behaviour for conditions outside the range for which practical experience is available. The majority of practical experience is derived from high and low pressure steam boilers in particular for conditions encountered in thermal power stations (Potter and Mann, 1961, Marsh, 1966). Contributions to the literature have however been obtained from experience with geothermal (Braithwaite, 1979) and nuclear power stations (Park and MacDonald, 1983). The protective properties of the duplex iron sulphide - magnetite films formed in steam environments containing H_2S, is sparsely documented in comparison, for example the corrosion performance of low carbon steel exposed to Ohaaki steam/condensate is as yet unknown. The most extensive systematic study has been undertaken for the high (1 MPa) pressure H_2S environments encountered in the Girdler-Sulphide process used in Canada for heavy water separation (Tewari *et al.*, 1979, Shoesmith *et al.*, 1980, Wikjord *et al.*, 1980). Practical experience is accumulating with geothermal steam containing H_2S, for example at Kawerau, however currently there have been no systematic studies of the variation of protection provided with practical operating parameters such as temperature, H_2S content, condensate pH and condensate velocity, all of which vary from one geothermal field to another or even within a geothermal field. Electrochemical Impedance Spectroscopy (EIS) and equivalent circuit theory was used to characterise both magnetite and iron sulphide-magnetite films grown on carbon steel at 160°C.

1.1 Magnetite Growth in High Temperature Aqueous Solutions

Studies of corrosion of iron and steel in high temperature aqueous solutions have shown that a duplex magnetite film is formed. There is a hard, crystalline outer layer which is the resutt of ferrous ions diffusing through the inner film and precipitating at the outer film/solution interface. The inner layer is formed from oxidation of ferrous ions at the metal/film interface and grows into the surface. The physical structure of the duplex iron sulphide - magnetite film formed in steam containing H_2S is similar in that the outer sulphide layer consists of well developed crystals most likely formed by the same process of ferrous ions diffusing through the inner film and precipitating at the film solution interface.

1.2 Electrochemical Impedance Spectroscopy and Equivalent Circuits

A brief explanation only of Electrochemical Impedance Spectroscopy (EIS) is provided here since a number of extensive reviews are available, e.g (Hladky et al., 1980, MacDonald and McKubre, 1981, Gabrielli and Keddam, 1992, Mansfeld, 1990). An electrochemical

interface can be modelled as a combination of electrical circuit elements, resistances, capacitances and inductances, each contributing to the total impedance, Z, of the interface. A model which is often used to represent a simple electrochemical interface is the Randles circuit, Figure 1.1, which consists of a solution resistance, R_s, a polarization resistance, R_p, and a double layer capacitance, C_{dl}. The application of a sinusoidal waveform to the interface, and measurement of the frequency response, allows the impedance of each element in the circuit to be determined. The waveform is applied over frequencies which range typically from 1 mHz to 100 kHz. The advantage of this method over traditional DC techniques, such as linear polarisation resistance, is that the solution resistance can be obtained from the high frequency end of the impedance spectrum, and therefore eliminated from subsequent calculations. This is especially important in low conductivity media. In addition, the amplitude of the applied waveform is small, typically 5 mV, so the interface is not disturbed by the polarisation process.

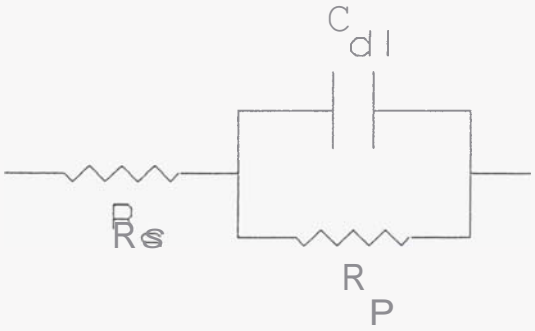

Figure 1.1 Simple Randies Circuit

The EIS data is typically presented in two ways. The first is as a Nyquist diagram, Figure 1.2(a), which plots the imaginary component of the interfacial impedance, -Z", against the real component, Z'. R_s is obtained from the high frequency end of the spectrum while extrapolation to lower frequencies gives R_p from which corrosion rates can be calculated. C_{dl} values are calculated from the mid-point of the semi-circle. The Bode plot presents the impedance spectra as the magnitude of the impedance, log |Z|, and the phase angle, ϕ, versus frequency, log f, Figure 1.2(b). R_s R_p and C_{dl} are determined graphically as shown. The slope of the curve, n, at f_{max} gives an indication of whether the corrosion process is activation controlled, n = -1, or diffusion controlled, n = -0.5. Both diagrams show the frequency response of a simple Randles circuit.

If the interface, and the impedance spectra of that interface, can be modelled using a simple circuit, graphical techniques of determining element impedances can be used. However, if the impedance

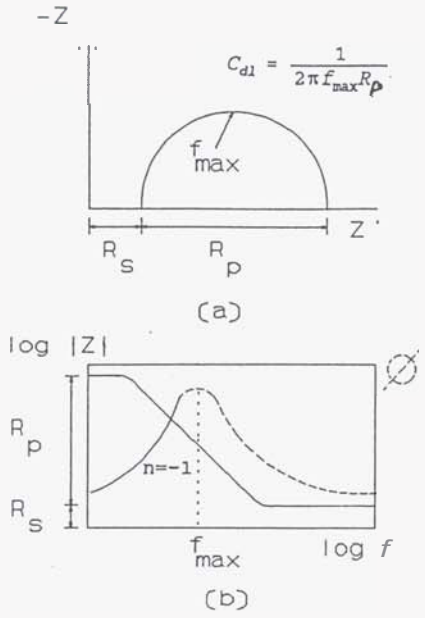

Figure 1.2 (a) Nyquist plot and (b) Bode plot of the Simple Randles Circuit in Figure 1.1

spectra are more complicated, other elements may have to be introduced into the equivalent circuit to ensure that the model accurately represents the frequency response of the corroding interface, and consequently the data may have to be analysed using more complicated techniques. EQUIVCRT (Boukamp, 1989) is a computer program written specifically for mathematical modelling of complex impedance spectra by equivalent circuits. Figure 1.3 gives the impedance spectrum and equivalent circuit of a more complex system. In this system, R_p includes a charge transfer resistance, R and a Warburg element, W. The Warburg component has a frequency dependent response and is characterised by a straight line at 45" in a Nyquist plot, or by a slope of -0.5 in plot of log |Z| vs log f. The Warburg element indicates a diffusion related process.

2. Experimental Method

The experiments were carried out in a recirculating autoclave system (Inman, 1991) for 10 days at T = 160°C and p = 6.5 bar. Both experiments, H_2S-free and H_2S-containing, were run at a pH of 6; 0.1 M Na_2SO_4 was added to improve solution conductivity. EIS scans were performed on a daily basis, and corrosion potentials were monitored continuously for the duration of each experiment. The electrochemical cell consisted of an AISI 1012 low carbon steel working electrode, a platinum auxiliary electrode and either a Ag/AgCl or a Ag/Ag_2S reference electrode, dependent

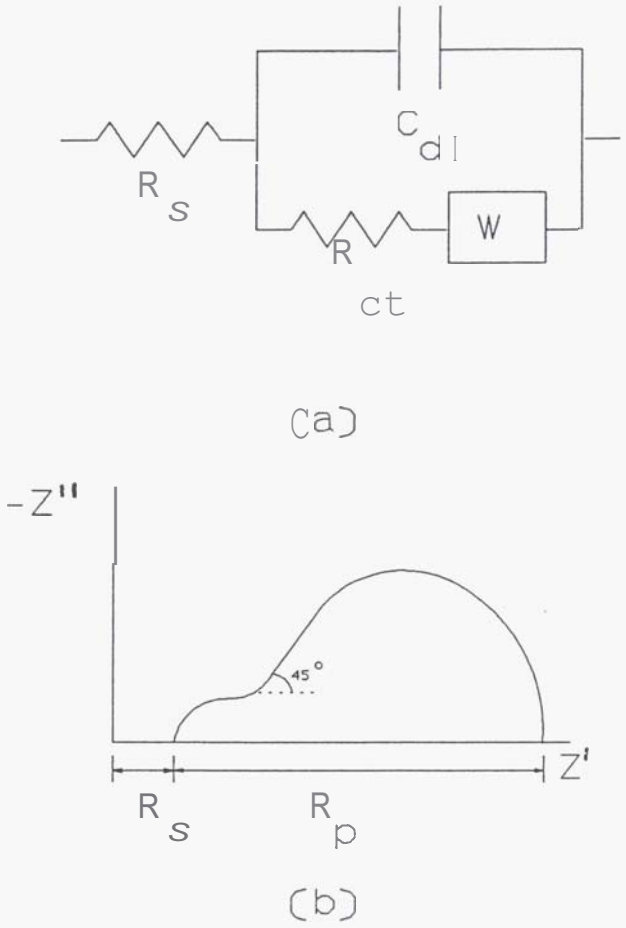

Figure 1.3 **(a) Equivalent Circuit and (b) Nyquist Plot for a System Under Diffusion Control**

upon whether or not H_2S was present in the system (MacDonald et *al.*, 1979b, Crowe and Tromans, 1986). 0.01 M NaCl was added to the solution to maintain the Ag/AgCl electrode. The reference electrode was located external to the autoclave and held at ambient temperature utilising a pressure balance design (MacDonald et *al.*, 1979a).

Impedance spectra were collected using a Model 5210 Lock-In Amplifier (EG&G Instruments Corp, 1992a) in conjunction with an EG&G PARC Model 273A Potentiostat (EG&G Instruments Corp, 1992b). The M388 Electrochemical Impedance software (EG&G Instruments Corp., 1989) was used to control the process. Corrosion potentials were measured using the Model 273A potentiostat in conjunction with the corrosion measurement software, Softcorr II (EG&G Instruments Corp., 1991). Weight loss coupons were also placed in the autoclave; these were prepared and cleaned in accordance with ASTM Standard G1-88 (ASTM, 1988).

3. Results and Discussion

Data from both experiments were analysed and fitted to a simple Randles circuit, and the results compared with weight loss data

3.1 Experiment 1: Magnetite Growth on Low Carbon Steel

Experiment 1 was a simulation of the conditions within the Wairakei steamlines. Figure 3.1 shows typical Bode and Nyquist plots of the data from Experiment 1. R_s, R_p and C_{dl} values were evaluated for each scan, and R_p was converted to corrosion rate data, which was plotted versus time, Figure 3.2. The material loss, 2.3 µm, was calculated from the area under the graph, and compares well with that determined from the coupon material loss of 2.1 µm. The average corrosion rate, 82.8 µm/yr, was also calculated from Figure 3.2. The fit of the Randles circuit to the impedance spectra from Experiment 1 was acceptable.

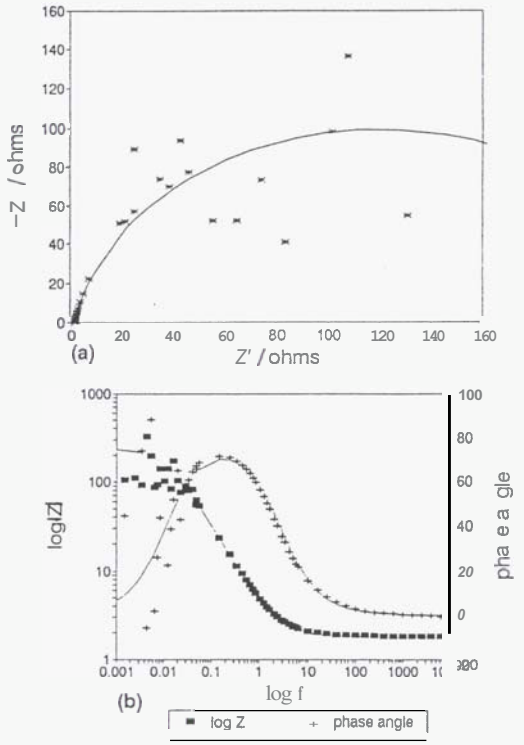

Figure 3.1 **Electrochemical Impedance Spectra of Low Carbon Steel at pH 6 and 160°C, in the absence of H_2S. Electrode Area = 4.8 cm²**

Corrosion potential data for Experiment 1 gave a final steady state corrosion potential of around -0.42 V vs SHE. The Pourbaix diagram for this system, Figure 3.3 (Johnson (1993)), predicts that the thermodynamically stable corrosion product at this potential is magnetite. This should be confirmed by later surface analysis.

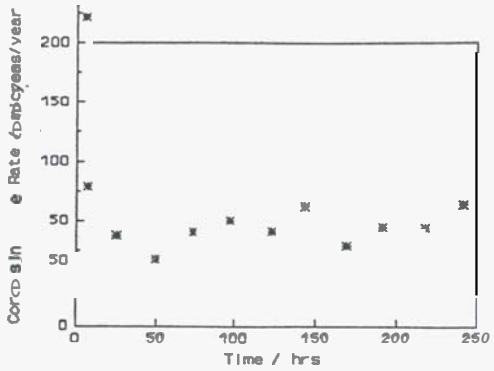

Figure 3.2 Corrosion Rate vs Time for Low Carbon Steel at pH 6 and 160°C, in the absence of H_2S.

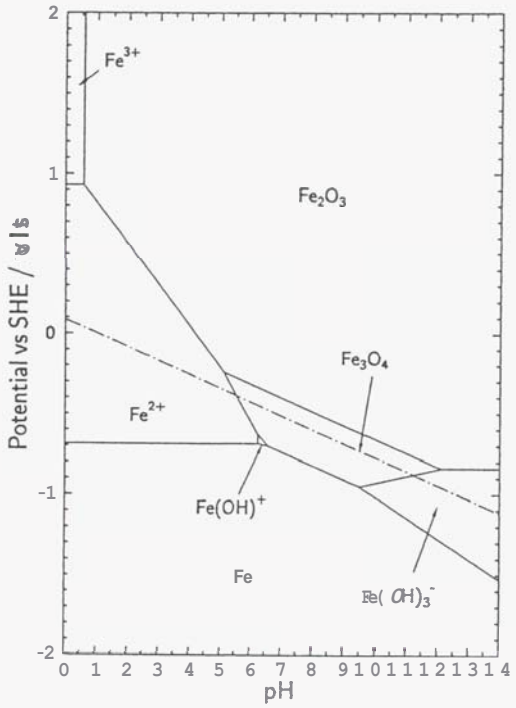

Figure 3.3 Pourbalx Diagram for the Fe-H_2O system at 160°C; $[Fe^{2+}]=10^{-5}$ mol/kg; $p_{H2}=10^{-2}$ atm.

3.2 Experiment 2: Iron Sulphide-Magnetite Film Growth on Low Carbon Steel

Experiment 2 was a simulation of the conditions within the Ohaaki steamlines; the concentration of H_2S in the solution was approximately 10^{-4} mol/kg. Typical impedance spectra from this experiment are given in Figure 3.4. The calculated R_p data obtained was converted to corrosion rate and plotted versus time, Figure 3.5. The penetration depth calculated from this set of data was 1.8 pm, whereas the weight loss coupon gave a material loss of around 2.5 µm. Although these values are of the same order of magnitude, it is evident that a more rigorous analysis, and more complex equivalent circuit, is required to adequately represent this system, as the spectra do

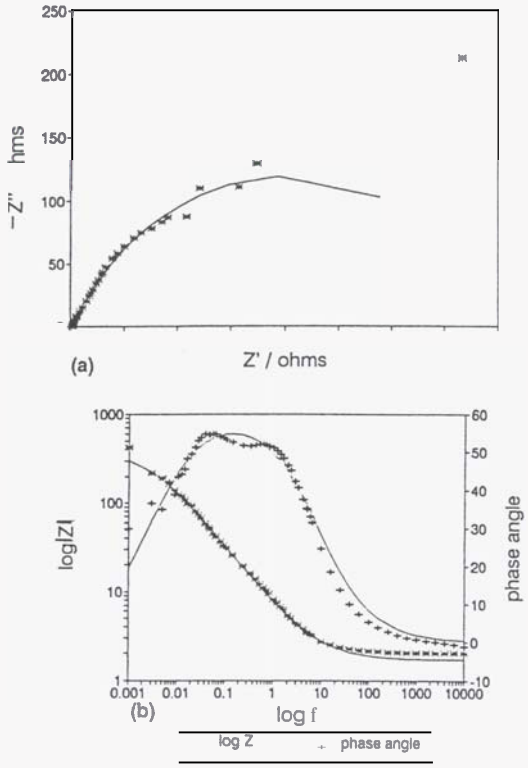

Figure 3.4 Electrochemical Impedance Spectra of low carbon steel at pH 6 and 160°C, for $[H_2S]=10^{-4}$ mol/kg. Electrode Area = 4.8 cm^2.

not appear to be those typical of a simple system. Additional circuit elements must be included which could take account of possible diffusion processes through the duplex film. Diffusion elements such as the Warburg component may contribute to R_p.

The corrosion potential data from this experiment showed a steady state corrosion potential of around

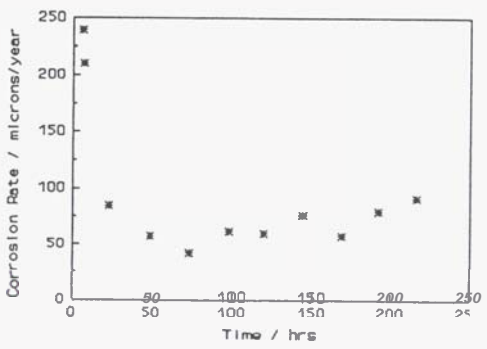

Figure 3.5 Corrosion Rate vs Time for low carbon steel at pH 6 and 160°C, for $[H_2S]=10^{-4}$ mol/kg.

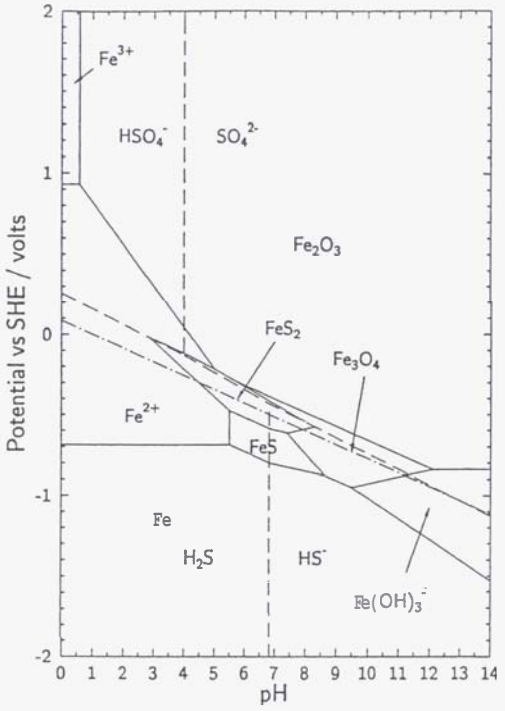

Figure 3.6 **Pourbaix Diagram for the Fe-S-H_2O system at 160°C; $[Fe^{2+}] = 10^{-5}$ mol/kg; $[H_2S] = 10^{-4}$ mol/kg; $p_{H2} = 10^{-2}$ atm.**

-0.36 V vs SHE. The Pourbaix diagram for this system, Figure 3.6, predicts that at this potential the thermodynamically stable corrosion product is pyrite. However, it is expected that given the short duration of the experiment, meta-stable corrosion products, namely the iron-rich compounds troilite and pyrrhotite, will have formed and would transform to pyriie if the experiment was run for a longer period of time (Lichti, 1983). Surface analysis, yet to be performed, should confirm the composition of the corrosion product specimens.

Overall, the impedance spectra from the magnetite and iron sulphide-magnetite systems are significantly different, and the equivalent circuit models used to represent the corroding interfaces will be dissimilar. Therefore, the capability to predict the corrosion performance of low carbon steel exposed to Ohaaki condensate cannot be based upon the knowledge of the simple magnetite system. More complex equivalent circuit modelling is required for the sulphide system to find a model which more closely fits the actual processes taking place. Once this has been accomplished, it will be easier to make a prediction of the corrosion performance of low carbon steel in contact with hot Ohaaki condensate.

4. Conclusions

The mechanism of pyrite film formation on carbon steel exposed to fluid containing H_2S, equivalent to that encountered at Ohaaki, is different from that observed for magnetite formed in an H_2S-free system. Consequently, the extensive practical experience gained from performance of carbon steel in low-H_2S steam can not be applied to systems such as Ohaaki, where iron sulphide passive films are encountered.

5. Acknowledgements

The authors wish to thank the Foundation for Research, Science and Technology for their assistance. The assistance of Barbara Webster is also appreciated.

6. References

ASTM G1-88. (1988). ***Standard Practice for Preparing, Cleaning and Evaluating Corrosion Test Specimens.***

Borshevska M., Lichti K.A. and Wilson P.T. (1982). The Relationship Between Corrosion Products and Corrosion Rates in Geothermal Steam. ***Proc. N.Z. Geothermal Workshop,*** 191-197.

Boukamp B.A. (1989). ***Equivalent Circuit (Equivcrt.pas) Users Manual,*** 2nd Ed. University of Twente, The Netherlands.

Braithwaite W.R. (1979). Corrosion in the 30 Inch Steam Pipelines at Wairakei Geothermal Field, American Chemical Society, Chemical Society of Japan, Honolulu Conf.

Crowe D.C. and Tromans D. (1986). The Silver Sulfide Reference Electrode for Use in Alkaline Sulfide Solutions. ***Corrosion,*** Vol. 42(7), 409-415.

EG&G Instruments Corp. (1989). ***Models*** 378 & ***388 Electrochemical Impedance Systems Instruction Manual.***

EG&G Instruments Corp. (1991). ***Model 352 Softcorr II Corrosion Measurement and Analysis Software User's Guide.***

EG&G Instruments Corp. (1992a). ***Model*** 5270 ***Lock-In Amplifier Instruction Manual.***

EG&G Instruments Corp. (1992b). ***Model*** 273A ***Potentiostat Instruction Manual.***

Foster P.K. and Tombs A. (1962). Corrosion by Hydrothermal Fluids. N.Z. *J. Sci.*, Vol. 5(1), 28–42.

Gabrielli C and Keddam M. (1992). Review of Applications of Impedance and Noise Analysis to Uniform and Localized Corrosion. ***Corrosion,*** Vol. 48(10), 794-811.

Hladky K., Callow LM. and Dawson J.L. (1980). Corrosion Rates From Impedance Measurements: An Introduction. ***Br. Corros. J.,*** Vol. 15(1), 20-25.

Inman M.E. (1991). Progress Report on the Study of the Passive Film formed on Mild Steel Exposed to Geothermal Condensate at T=160°C. Report No. RI 3210, DSIR Industrial Development, Wellington.

Johnson C.A. (1993). User Guide to Program 'Pourbaix' for Calculating and Plotting Pourbaix Diagrams. IRL Report No. 18013.31, Industrial Research Ltd, Wellington.

Lichti K.A. and Wilson P.T. (1983). Materials Testing in Geothermal Steam. ***Proc.*** of ***the Int. Symposium on Solving Corrosion and Scaling Problems in Geothermal Systems,*** San Francisco, California, January 17-20, 269-284.

MacDonald D.D., Scott A.C. and Wentrcek P. (1979a). External Reference Electrodes for Use in High Temperature Aqueous Systems. ***J. Electrochem. Soc.,*** Vol. 126(6), 908-911.

MacDonald D.D., Scott A.C. and Wentrcek P. (1979b). Silver-Silver Chloride Thermocells and Thermal Liquid Junction Potentials for Potassium Chloride Solutions at Elevated Temperatures. J. ***Electrochem. Soc.,*** Vol. 126(9), 1618-1624.

MacDonald D.D. and McKubre M.C.H. (1981). Electrochemical Impedance Techniques in Corrosion Science. ***Electrochemical Corrosion Testing, ASTM STP 727,*** F. Mansfeld and U. Bertocci (Eds)., American Society for Testing and Materials, 110-149.

MacDonald D.D. (1992). The Point Defect Model for the Passive State. ***J. Electrochem. Soc.,*** Vol. 139(12), ***3434-***3449.

Marshall T. and Hugill A.J. (1957). Corrosion by Low Pressure Geothermal Steam. ***Corrosion,*** Vol. 13, 329t-337t.

Mansfeld F. (1990). Electrochemical Impedance Spectroscopy (EIS) as a New Tool for Investigating Methods of Corrosion Protection. ***Electrochimica Acta,*** Vol. 35(10), 1533-1544.

Marsh T. (1966). The Morphology of Magnetite Growth on Mild Steel in Alkaline Solutions at 316°C. J. ***Electrochem. Soc.,*** Vol. 113(4), 313-318.

Park J.R. and MacDonald D.D. (1983), Impedance Studies of the Growth of Porous Magnetite Films on Carbon Steel in High Temperature Aqueous Systems. ***Corrosion Science,*** Vol. 23(4), 295315.

Potter E.C. and Mann G.M.W. (1961). Oxidation of Mild Steel in High-temperature Aqueous Systems. ***Proc. First Int. Congr. on Metallic Corrosion,*** Butterworths, London, 49-55.

Potter E.C. and Mann G.M.W. (1965). The Fast Linear Growth of Magnetite on Mild Steel in High-Temperature Aqueous Conditions. ***Br. Corros. J.,*** Vol. 1, 26-35.

Robertson J. (1989). The Mechanism of High Temperature Aqueous Corrosion of Steel. ***Corrosion Science,*** Vol. 29(11/12), 1275-1291.

Sato N. (1989). Towards a More Fundamental Understanding of Corrosion Processes. ***Corrosion,*** Vol. 45(5), 354-368.

Shoesmith D.W., Taylor P., Bailey M.G. and Owen D.G. (1980). The Formation of Ferrous Monosulphide Polymorphs during the Corrosion of Iron by Aqueous Hydrogen Sulphide at 21°C. J. ***Electrochem. Soc.,*** Vol. 127(5), 1007-1015.

Tewari P.H., Bailey M.G. and Campbell A.B. (1979). The Erosion- Corrosion of Carbon Steel in Aqueous H_2S Solutions up to 120°C and 1.6 MPa Pressure. ***Corrosion Science,*** Vol. 19, 573-585.

Wikjord A.G., Rummery T.E., Doern F.E. and Owen D.G. (1980). Corrosion and Deposition during the Exposure of Carbon Steel to Hydrogen Sulphide-Water Solutions. ***Corrosion Science,*** Vol. 20, 651-671.